Proc. Natl. Acad. Sci. USA
Vol. 91, pp. 10029–10033, October 1994
Biophysics

Fluctuation of the number of particles deposited on a flat surface by a random sequential adsorption mechanism

(simulation/correlation/finite size effects)

B. SENGER*†, P. SCHAAF‡§, J.-C. VOEGEL*, P. WOJTASZCZYK‡, AND H. REISS¶

*Institut National de la Santé et de la Recherche Médicale, CJF 92-04, Centre de Recherches Odontologiques, Université Louis Pasteur, 1, place de l'Hôpital, 67000 Strasbourg, France; ‡Institut Charles Sadron, 6, rue Boussingault, 67083 Strasbourg Cedex, France; §Ecole Européenne des Hautes Etudes des Industries Chimiques, Unité de Recherche Associée 405 (Centre National de la Recherche Scientifique), BP 296F, 1, rue Blaise Pascal, 67008 Strasbourg Cedex, France; and ¶Department of Chemistry and Biochemistry, University of California, 405 Hilgard Avenue, Los Angeles, CA 90024-1569

Contributed by H. Reiss, July 5, 1994

ABSTRACT **The problem of the fluctuations of the number n of particles adsorbed on surfaces through a random sequential adsorption process is discussed. Attention is paid, in particular, to the effect of the size of the adsorbing surfaces upon the variance $\sigma^2(n)$ of this number. On the basis of computer simulations, it is shown that $\sigma^2(n)$ is not proportional to the area a of the surface but can be written as a sum of three contributions, which are proportional to a, $a^{1/2}$, and a^0. A theoretical estimate based on the relation between the radial distribution function $g(r)$ and the fluctuation is presented and provides a basis for these findings. This analysis is of general validity and can, in particular, also be applied to the equilibrium case (in the absence of a phase transition) and to the ballistic deposition process.**

Many adsorption (or adhesion) processes of large molecules (or particles) on solid surfaces are irreversible in the sense that, once adsorbed, the molecules neither diffuse on nor desorb from the surface. Moreover, surface exclusion effects play an important role during the adsorption mechanism. The analysis of such irreversible processes has been widely investigated from a theoretical point of view during the last years, and different models have been proposed to describe them. Among them, the most popular are the random sequential adsorption (RSA) model (1) and the ballistic model (2). Attention has been focused mainly on the prediction of the adsorption kinetics (3, 4) and on the behavior of the systems at or near the "jamming limit" (5–8).

On the other hand, only a few experimental studies have been performed to investigate the range of validity of these models (9–13). Adsorption kinetics were analyzed in the case of protein solutions (9, 11), and the radial distribution functions were determined in the case of particle adhesion. The later systems were studied by means of optical microscopy (12, 13). The most recent experiments have shown that not only does the radial distribution function contain information about the adsorption mechanism but so does the fluctuation of the number of particles in an assembly of small systems, each corresponding to a portion of a larger surface upon which particles were adsorbed (13). Understanding these fluctuations is thus of great importance to the interpretation of the experiments. Moreover, fluctuations also play an important role in equilibrium statistical mechanics and are thus of considerable interest to delineate the common features of both situations. Finally, the systems corresponding to the pictures obtained via optical microscopy for the purpose of determining the radial distribution functions were small, in the sense that near the jamming limit, they typically involved 500 particles. Border effects can thus play an important role in the distribution function of such small systems.

Despite the importance of the fluctuations, only two theoretical studies devoted to this problem are known to the authors (13, 14). In their pioneering work on the RSA model, Cohen and Reiss (14) have determined exactly the fluctuation of the number of adsorbed dimers on lattice systems of *any size*. This approach seems, however, not generalizable to deposition processes on a plane. More recently, another approach to this problem has been proposed in connection with the experimental results already mentioned (13). A master equation system was derived whose resolution allowed the precise prediction of fluctuations up to a coverage of 25% (the jamming limit coverage is of the order of 0.55 for RSA and 0.61 for the ballistic model). Unfortunately, this scheme is not easily extended to accurate predictions over the full coverage range.

In this article, we therefore analyze the fluctuation of the number of particles in *small* systems by means of computer simulation using the RSA model. The problem of the influence of the size of the system on the fluctuation is addressed. In particular, analytical expressions for the variance $\sigma^2(n)$ of the number n of adsorbed particles are derived such that $\sigma^2(n)$ can be *predicted* for a system of any size. We also propose, for the RSA model, an approximate expression for the variance of systems in which edge effects can be neglected (large systems). This expression is based on the connection between the fluctuation and the radial distribution function $g(r)$, a connection used recently for large one-dimensional systems for the RSA case (15).

Simulation Procedure

The simulation model is the usual RSA model describing the deposition of particles on a collector (generally a flat surface or a straight line) (1). This deposition occurs at a randomly selected position subject only to the restriction that the deposited particle does not overlap a previously adsorbed one. If overlapping occurs, the particle is rejected and the deposit of a new one is attempted. Once adsorbed, an object is assumed to be permanently fixed in place. Periodic boundary conditions are applied at the edges of the collector. In the particular case of the square collectors studied here, each deposited particle is replicated in the eight neighboring squares. In this way one simulates an infinitely large area, and edge effects are substantially reduced. At the jamming limit—i.e., when no further particle can be added to the surface—the coverage $\theta(\infty)$ is on the average equal to 0.547 for disks (1). It is also well known that large samples of surfaces are necessary to obtain an accurate estimate of this

The publication costs of this article were defrayed in part by page charge payment. This article must therefore be hereby marked "*advertisement*" in accordance with 18 U.S.C. §1734 solely to indicate this fact.

Abbreviation: RSA, random sequential adsorption.

†To whom reprint requests should be addressed.

limiting coverage, since $\theta(\infty)$ varies from one small surface to another.

Large square surfaces were filled with disks up to a coverage of about 0.5. Coverages ranging from 0.5 to $\theta(\infty)$ were not investigated due to prohibitive computer time. The center of a disk coincides with the node of a fine-mesh square grid whose periodicity is arbitrarily taken as the unit of length. Throughout this article, all distances are expressed in this arbitrary unit. The large surfaces of area A were subdivided virtually into ν smaller square subsystems of area $a=A/\nu$. At the border of the subsystems no periodic boundary conditions apply. A particle in the vicinity of the border of a subsystem has thus the same environment as all the other particles of the large system (Fig. 1). During the filling procedure, the number n_i of disk centers located in the ith subsystem was determined as a function of the average coverage θ. The variance $\sigma^2(n)$, which is *a priori* a function of A, ν, and θ, is then defined by

$$\sigma^2(n) = \frac{1}{\nu}\sum_{i=1}^{\nu} n_i^2 - \left(\frac{1}{\nu}\sum_{i=1}^{\nu} n_i\right)^2. \qquad [1]$$

Simulation Results

A first set of results was obtained on the basis of square surfaces of side $A^{1/2} = 1024, 2048, 4096, 8192, 16{,}384, 32{,}768,$ and 65,536 covered by disks of radii $R = 50$, and subdivided into $\nu = 64$ small subsystems each. Samples of 1000 and 500 surfaces were accumulated for $A^{1/2} \leq 16{,}384$ and for $A^{1/2} =$ 32,768 and 65,536, respectively.

For a very low coverage (i.e., for a very small number N of particles deposited on a surface of area A), the probability of finding n disks on one of the ν subsystems essentially follows a binomial law. The corresponding variance $\sigma_b^2(n)$ is given by

$$\sigma_b^2(n) = \frac{A\theta}{\nu\pi R^2}\frac{\nu-1}{\nu} \equiv \frac{a\theta}{\pi R^2}\frac{\nu-1}{\nu}, \qquad [2]$$

where the subscript "b" refers to binomial. The variances derived from the simulations were therefore multiplied by $\nu\pi R^2/(\nu-1)a$, leading to reduced variances, denoted y in the following:

$$y = \frac{\nu\pi R^2}{(\nu-1)a}\sigma^2(n). \qquad [3]$$

The reduced variances obtained in this way are shown in Fig. 2 for different values of the area a of the subsystem. It is clearly apparent that y does indeed behave as θ as the coverage tends to 0, confirming the prediction of a binomial law at low coverage. More interesting is the variation of y with the surface area a of the subsystems (or, in this case, with the area A of the large system). This variation proves that $\sigma^2(n)$ is not proportional to the area a (or A) as might be expected at first thought. Indeed, if this were the case, the curves corresponding to the seven values of a (or A) would merge into a single curve. Furthermore, it should be indicated that y does not vanish as θ approaches the jamming limit, $\theta(\infty)$. This stems from the fact that the ν subsystems do not all saturate at the same coverage. $\theta(\infty)$ is the *average* of the individual jamming coverages and is not a common limit for all subsystems.

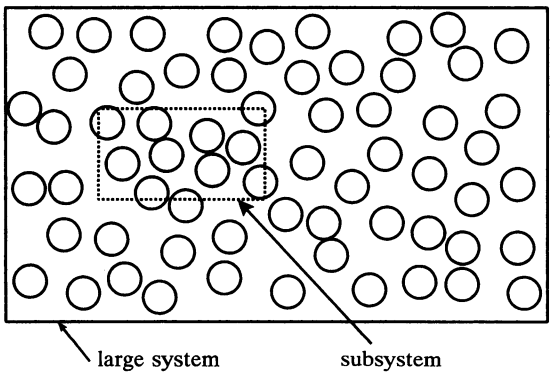

FIG. 1. Schematic representation of a large system, including a small subsystem (not drawn to scale), covered with disks or spheres. Periodic boundary conditions apply at the perimeter of the large system; in contrast, the subsystem is not surrounded by walls.

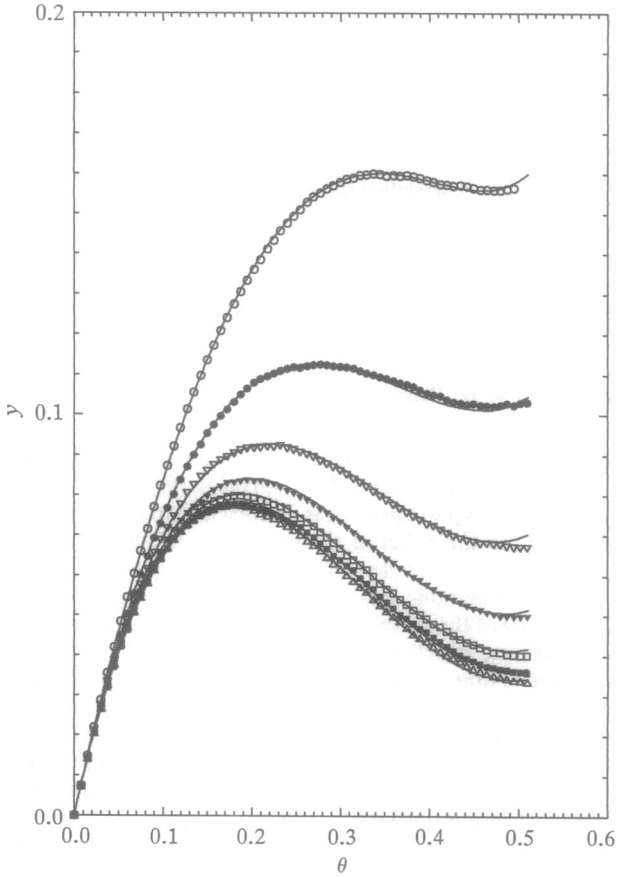

FIG. 2. Reduced variance y as a function of the coverage θ. Each curve corresponds to a large square surface of area A subdivided into $\nu = 64$ small square surfaces. From top to bottom: $A^{1/2} = 1024, 2048, 4096, 8192, 16{,}384, 32{,}768,$ and 65,536. The solid lines represent their fit by $y = y_0 + y_1\,(a/\pi R^2)^{-1/2} + y_2(a/\pi R^2)^{-1}$, where y_0, y_1, and y_2 are the polynomials drawn in Fig. 4 and given by Eqs. **14**, **18**, and **19**.

To verify whether it is the large system or the subsystem that is responsible for the dependence of variance on size, the simulations were repeated for $A^{1/2} = 2048, 4096, 8192, 16{,}384, 32{,}768,$ and 65,536 and $\nu = 256$. These results were compared to the preceding simulations. For example, the normalized variance y corresponding to ($A^{1/2} = 16{,}384$, $\nu = 256$) was compared to y corresponding to ($A^{1/2} = 8192$, $\nu = 64$). No difference in y could be detected when the size a of the subsystem remained constant, although the area A of the large system was varied by a factor of 4.

Finally, the fact that subsystems derived from the same large system could have a common border might be responsible for the observed size dependence. To show that this was not the case, the variance corresponding to the preceding simulations was redetermined using only half of the $\nu = 256$ subsystems, the selected ones being located on the large

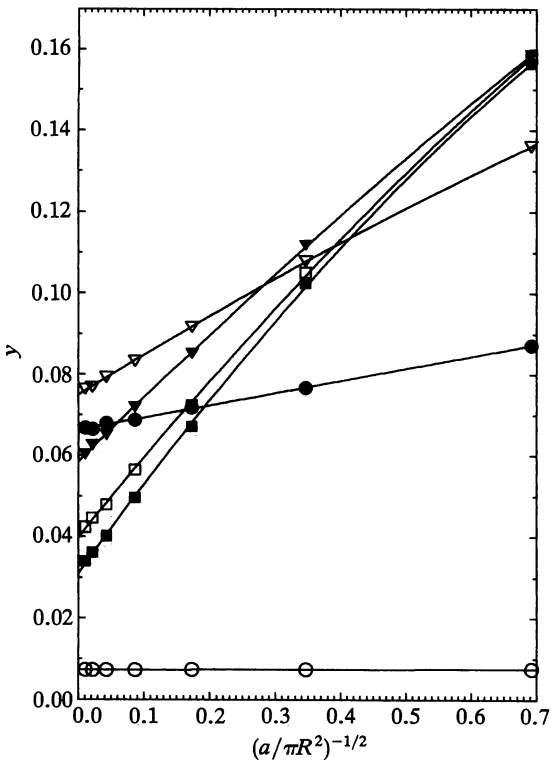

FIG. 3. Reduced variance y as a function of $(a/\pi R^2)^{-1/2}$; the large surfaces of area A, covered by disks of radius R, are subdivided into 64 subsystems of area a. Each curve corresponds to a fixed value of the coverage θ selected among the 66 values recorded between 7.49 $\times 10^{-3}$ up to 0.4943: $\theta \approx 0.0749$ (○), 0.105 (●), 0.202 (▽), 0.307 (▼), 0.404 (□), 0.494 (■). The solid lines are the least-squares fits of $y = y_0 + y_1(a/\pi R^2)^{-1/2} + y_2(a/\pi R^2)^{-1}$ to the data.

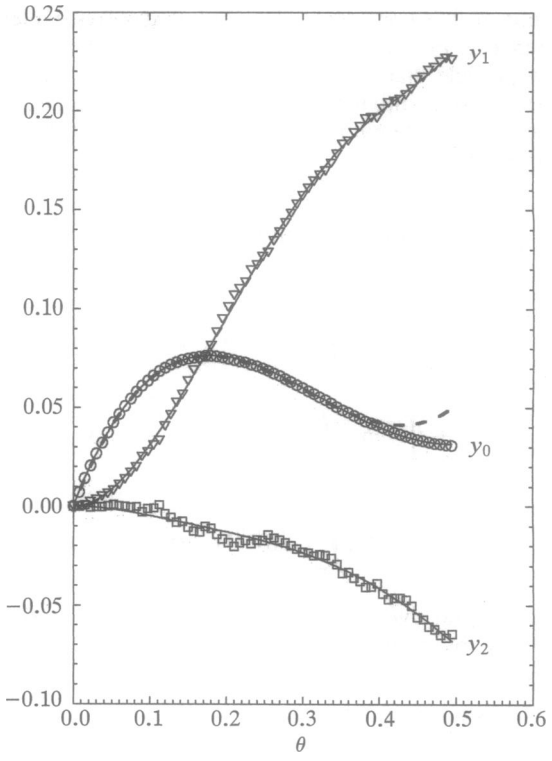

FIG. 4. Variation of the parameters y_0 (○), y_1 (▽), and y_2 (□) (see also Fig. 3) with the coverage θ, together with the respective fifth-degree polynomial fits (Eqs. **14**, **18**, and **19**; solid lines). The dashed line represents the theoretical third-order approximation of y_0 (Eq. **13**).

system as the squares of one color on a chessboard. Again, y remained unaltered. Thus, the size effect on the variance is not due to the common border shared by different subsystems.

The variance $\sigma^2(n)$ is thus a function of the coverage θ and the size of the subsystem a (or A/ν). The same holds for the reduced variance y. Instead of representing y as a function of θ for various values of A or a, it is more convenient to represent y as a function of the size of the subsystem for selected values of θ between zero and ≈0.5 (Fig. 3). The most natural variable is the square root of the "packing fraction" $(a/\pi R^2)^{-1/2}$ rather than a itself, since y equals θ and is independent of this fraction at low coverage. As θ increases, however, an evident departure from θ can be observed, and y carries over into a quadratic function of $(a/\pi R^2)^{-1/2}$. As the data suggest, and as we make plausible later, y can be written as the sum of three contributions:

$$y = y_0 + y_1(a/\pi R^2)^{-1/2} + y_2(a/\pi R^2)^{-1}. \qquad [4]$$

Extrapolation to infinitely large surfaces leads to $y(a = \infty) = y_0$. The functions y_0, y_1, and y_2 of θ (Fig. 4) can be accurately represented by polynomials of the fifth degree fitted by a least-squares method applied to the data of Fig. 3. However, several fitting parameters can be estimated theoretically, as explained in the following section.

Theoretical Considerations

We present a theory for the dependence of y on the size of the subsystem. We denote by $\rho(\mathbf{r})$ the density of particle centers, in a particular subsystem at $\mathbf{r}$. The notation $\langle\ \rangle$ indicates an average taken over an ensemble of subsystems. $\langle\rho(\mathbf{r})\rangle$ is thus the mean density ρ of the particles adsorbed on the subsystem. Following Landau and Lifchitz (16), we also have

$$\langle n^2\rangle = \int_{\text{sub}}\int_{\text{sub}} \langle\rho(\mathbf{r}_1)\rho(\mathbf{r}_2)\rangle d\mathbf{r}_1 d\mathbf{r}_2, \qquad [5]$$

where "sub" refers to the subsystem. $\langle\rho(\mathbf{r}_1)\rho(\mathbf{r}_2)\rangle = \rho\delta(\mathbf{r}_1 - \mathbf{r}_2) + \rho^2 g^{(2)}(\mathbf{r}_1, \mathbf{r}_2)$, where $g^{(2)}(\mathbf{r}_1, \mathbf{r}_2)$ is the pair correlation function (17), so that Eq. **5** combined with $\langle n\rangle = \rho a$ leads to

$$\langle n^2\rangle - \langle n\rangle^2 = \rho a + \rho^2 \int_{\text{sub}}\int_{\text{sub}} (g^{(2)}(\mathbf{r}_1, \mathbf{r}_2) - 1) d\mathbf{r}_1 d\mathbf{r}_2. \qquad [6]$$

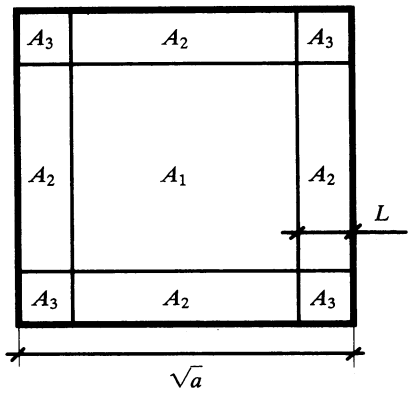

FIG. 5. Schematic representation of a small square subsystem of area a, subdivided into three types of regions: "core" (A_1), "margins" (A_2), and "corners" (A_3); each of them has a specific contribution to the observed variance of the number of particles deposited on the subsystem.

Assume, as it is commonly observed, that $g^{(2)}(\mathbf{r}_1, \mathbf{r}_2)$ tends to 1 when $|\mathbf{r}_1 - \mathbf{r}_2|$ becomes of the order of a distance L (usually a few particle diameters). One can then divide the area of each subsystem into three domains A_1, A_2, and A_3, as defined in Fig. 5. The integral in Eq. **6** can then be written as a sum of three terms:

$$\int_{\text{sub}}\int_{\text{sub}} (g^{(2)}(\mathbf{r}_1, \mathbf{r}_2) - 1)d\mathbf{r}_1 d\mathbf{r}_2$$

$$= \int_{A_1} d\mathbf{r}_1 \int_{\text{sub}} (g^{(2)}(\mathbf{r}_1, \mathbf{r}_{12}) - 1)d\mathbf{r}_{12}$$

$$+ \int_{A_2} d\mathbf{r}_1 \int_{\text{sub}} (g^{(2)}(\mathbf{r}_1, \mathbf{r}_{12}) - 1)d\mathbf{r}_{12}$$

$$+ \int_{A_3} d\mathbf{r}_1 \int_{\text{sub}} (g^{(2)}(\mathbf{r}_1, \mathbf{r}_{12}) - 1)d\mathbf{r}_{12}. \quad [7]$$

In the integral over A_1, all the positions $\mathbf{r}_1$ are statistically equivalent by definition of A_1. Thus this term may be expressed by

$$\int_{A_1} d\mathbf{r}_1 \int_{\text{sub}} (g^{(2)}(\mathbf{r}_1, \mathbf{r}_{12}) - 1)d\mathbf{r}_{12}$$

$$= (\sqrt{a} - 2L)^2 \int_0^\infty (g^{(2)}(\mathbf{r}) - 1)d\mathbf{r} = zs(\sqrt{a} - 2L)^2 C_0(\theta), \quad [8]$$

which defines the function $C_0(\theta)$. In the second and third integrals, integrated respectively over A_2 and A_3, all the positions of $\mathbf{r}_1$ are not statistically equivalent. It is easily verified, however, that the second integral takes the form $4(\sqrt{a} - 2L)C_1(\theta, L)$, where $C_1(\theta, L)$ is a function of θ and L but not of the size of the subsystem, and that the third integral may also be expressed as a function $C_2(\theta, L)$ of θ and L alone as well. The variance takes then the general form:

$$\langle n^2\rangle - \langle n\rangle^2 = \rho a + \rho^2(\sqrt{a} - 2L)^2 C_0(\theta)$$

$$+ \rho^2 4(\sqrt{a} - 2L)C_1(\theta, L) + \rho^2 C_2(\theta, L). \quad [9]$$

This result provides the basis for the form of the reduced variance y postulated previously (Eq. **4**).

For the RSA case, $g^{(2)}(\mathbf{r})$ is known as a diagrammatic expansion in the density ρ (18). Out to the first order in the density, it is given by

$$\begin{cases} g^{(2)}(r) = 1 + \dfrac{2}{3}\rho B_2(r), & \text{for } r \geq d \\ g^{(2)}(r) = 0, & \text{for } r < d, \end{cases} \quad [10]$$

where $B_2(r)$ is the common area of two disks of radii $d = 2R$ separated by a distance r. One then gets

$$\int_0^\infty (g^{(2)}(r) - 1)2\pi\, r dr = -\pi d^2 + \frac{2}{3}\rho \int_0^\infty B_2(r)2\pi\, r dr. \quad [11]$$

From ref. 3, one obtains directly

$$\int_0^\infty B_2(r)2\pi\, r dr = \frac{12\sqrt{3}}{\pi}\left(\frac{\pi d^2}{4}\right)^2, \quad [12]$$

and this leads to

$$y_0 = \theta - 4\theta^2 + \frac{24}{\pi\sqrt{3}}\theta^3 + 0(\theta^4). \quad [13]$$

Fig. 4 exhibits y_0 both derived from simulation together with the third-order expression, Eq. **13**. Clearly, this approximation is accurate up to $\theta \approx 0.38$. Higher order terms could be obtained by using the same procedure, but the values of diagrams out to order 4 would be needed. Instead, we used a fitting procedure to determine the higher order terms. This leads to

$$y_0 = \theta - 4\theta^2 + \frac{24}{\pi\sqrt{3}}\theta^3 + 0.823992\theta^4 - 2.28279\theta^5. \quad [14]$$

Eq. **14** is a convenient and accurate means (Fig. 4) to represent the reduced variance in the asymptotic regime ($a \rightarrow \infty$).

The same kind of analysis can be performed in order to estimate the contribution of the areas A_2 to the variance. The relevant integral is

$$I_2 = \int_{A_2}\int_{\text{sub}} (g^{(2)}(\mathbf{r}_1, \mathbf{r}_2) - 1)d\mathbf{r}_1 d\mathbf{r}_2. \quad [15]$$

From elementary geometric considerations, it can be shown that this integral takes the form

$$I_2 = 4(\sqrt{a} - 2L)\int_0^L \left\{ \int_0^x (g^{(2)}(r) - 1)2\pi\, r dr \right.$$

$$\left. + 2\int_x^\infty (g^{(2)}(r) - 1)\left(\pi - \arccos\left(\frac{x}{r}\right)\right) r dr \right\} dx. \quad [16]$$

These integrals can be performed analytically to the lowest order in the density ρ. After a tedious but straightforward calculation one obtains

$$y_1 = \frac{64}{3\pi^{3/2}}\theta^2 + 0(\theta^3). \quad [17]$$

Additional terms can be evaluated by numerical integration of more complicated expressions. On the other hand, using a polynomial fitting procedure provides a good approximation of these terms. In this way, y_1 may be estimated to the fifth order by (Fig. 4):

$$y_1 = \frac{64}{3\pi^{3/2}}\theta^2 - 7.13566\theta^3 - 2.22364\theta^4 + 9.75881\theta^5. \quad [18]$$

Finally, the best polynomial fit to y_2 leads to (Fig. 4):

$$y_2 = -0.777088\theta^2 + 3.71684\theta^3 - 8.48006\theta^4 + 6.06697\theta^5. \quad [19]$$

It may be noted that since y must behave as θ at low coverage, no θ term was included in y_2. The fitting parameters were otherwise free. Inserting the polynomials from Eqs. **14, 18,** and **19** into Eq. **4** leads to an analytical expression for y containing both θ and a. The solid curves in Fig. 2 demonstrate that the accuracy of this analytical expression of y is remarkable and thus attests the accuracy of the hypothesis that, for a given coverage, y can be approximated by a polynomial of second degree in $(a/\pi R^2)^{-1/2}$.

Finally, it can also be pointed out that the first terms in y_0 and y_1 are equivalent for all the deposition processes of hard spheres on surfaces and also for equilibrium systems in the

absence of a phase transition. It thus constitutes a general result that goes far beyond the RSA case.

Conclusions

We have examined the problem of the fluctuation of the number of particles on a small subsystem of a large system generated through an RSA algorithm. Both computer simulation and theoretical estimate indicate that the variance of the number of particles adsorbed on a subsystem is the sum of three contributions: one proportional to the size a of the subsystem, another proportional to $a^{1/2}$, and still another that is constant. This result appears to be applicable not only to the RSA case but for most two-dimensional systems. Contributions to these different terms were estimated, by means of theory, for the RSA case. The theory is well defined and is confirmed by simulation. However, it is questionable under the conditions of phase transition. Expressions obtained by fitting empirical functions to the simulation results are also given so that for the RSA case, the variance for any system can be predicted.

The authors are indebted to Professor M. Rubi and Drs. G. Koper and I. Pagonabarraga for fruitful discussions. They acknowledge especially Professor D. Bedeaux for drawing their attention to the relation between the fluctuations and the correlation function. This work was supported in part by the Institut National de la Santé et de la Recherche Médicale (contract no. CJF 92-04), the Commission of the European Communities [contract no. SC1/CT/910696(TSTS)], and the North Atlantic Treaty Organization (contract no. 890872). P. Schaaf and H. Reiss acknowledge the Centre National de la Recherche Scientifique (CNRS) and the National Science Foundation (NSF) for an NSF/CNRS grant supporting part of this work.

1. Hinrichsen, E. L., Feder, J. & Jøssang, T. (1986) *J. Stat. Phys.* **44,** 793–827.
2. Jullien, R. & Meakin, P. (1992) *J. Phys. A: Math. Gen.* **25,** L189–L194.
3. Schaaf, P. & Talbot, J. (1989) *J. Chem. Phys.* **97,** 4401–4409.
4. Evans, J. W. (1989) *Phys. Rev. Lett.* **62,** 2642.
5. Pomeau, Y. (1980) *J. Phys. A: Math. Gen.* **13,** L193–L196.
6. Swendsen, R. H. (1981) *Phys. Rev. A: Gen. Phys.* **24,** 504–508.
7. Vigil, R. D. & Ziff, R. M. (1990) *J. Chem. Phys.* **93,** 8270–8272.
8. Talbot, J., Tarjus, G. & Schaaf, P. (1989) *Phys. Rev. A: Gen. Phys.* **40,** 4808–4811.
9. Feder, J. & Giaever, I. (1980) *J. Colloid Interface Sci.* **78,** 144–154.
10. Onoda, G. Y. & Liniger, E. G. (1986) *Phys. Rev. A: Gen. Phys.* **33,** 715–716.
11. Ramsden, J. J. (1993) *Phys. Rev. Lett.* **71,** 295–298.
12. Adamczyk, Z., Zembala, M., Siwek, B. & Warszynski, P. (1990) *J. Colloid Interface Sci.* **140,** 123–137.
13. Wojtaszczyk, P., Schaaf, P., Senger, B., Zembala, M. & Voegel, J.-C. (1993) *J. Chem. Phys.* **99,** 7198–7208.
14. Cohen, E. R. & Reiss, H. (1963) *J. Chem. Phys.* **38,** 680–691.
15. Bonnier, B., Boyer, D. & Viot, P. (1994) *J. Phys. A: Math. Gen.* **27,** 3671–3682.
16. Landau, L. & Lifchitz, E. (1967) *Physique Statistique* (Editions Mir, Moscow), pp. 434–437.
17. Hill, T. L. (1987) *Statistical Mechanics and Selected Applications* (Dover, New York).
18. Tarjus, G., Schaaf, P. & Talbot, J. (1991) *J. Stat. Phys.* **63,** 167–202.